15TH IEA HEAT PUMP CONFERENCE
MAY 26–29, 2026 | HOFBURG
VIENNA 2026
DECARBONISATION THROUGH INNOVATION

Transcritical CO_2 high temperature heat pump for the brewery industry

G. Calvo[a], J.I. Linares[a,*], E. Arenas[b,c], J.R. Pérez-Domínguez[b,c]

[a] Repsol Foundation Chair in Energy Transition, Comillas Pontifical University, Alberto Aguilera 25, Madrid 28015, Spain
[b] Rafael Mariño Chair in New Energy Technologies, Comillas Pontifical University, Alberto Aguilera 25, Madrid 28015, Spain
[c]Institute for Research in Technology, Comillas Pontifical University, , Rey Francisco 4, Madrid 28008, Spain

Abstract

The brewing industry requires processes at different thermal levels, combining simultaneous heating and cooling demands. A typical process includes wort cooling and water preheating, usually achieved via a heat recovery heat exchanger, along with steam generation for adjunct and mash kettles using a conventional boiler. Water is sourced from the distribution network and pre-cooled in chillers before entering the recuperator to cool the wort to the desired temperature. While part of the steam demand is met using self-produced biogas, additional fuel—typically natural gas—is required.
As an alternative for decarbonizing the process, a high-temperature heat pump is proposed to integrate three thermal demands: inlet-water heating, wort cooling, and steam production. The proposed solution is a transcritical CO_2 heat pump equipped with a recuperator that divides the gas cooler into two sections: one for heating thermal oil (stored for subsequent steam generation), and another for preheating the inlet water. The heat pump's evaporator cools the wort, which acts as the thermal source.
The inlet water enters the system at 8°C to 24°C and is heated to 90°C. The thermal oil enters the heat pump at temperatures between 136°C and 155°C and returns to storage at 343°C to 269°C. The wort is cooled from 98°C to 10°C, with a thermal load ranging from 9.2 to 18.4 MW_{th}. The seasonal coefficient of performance (COP) for combined heating and cooling is 4.82. The levelized cost of energy (through thermal oil heating) ranges from 67.59 to 78.15 €/MWh_{th}. The payback period varies from 5.31 to 14.7 years, depending on specific economic assumptions.

Keywords: High temperature heat pumps; Transcritical reverse cycle; Carbon dioxide as working fluid; Heat electrification

1. Introduction

Medium-temperature heat demands in breweries (120-200°C)—dominated by wort boiling and evaporation, pasteurization, clean-in-place (CIP), and site-thermal utilities—are increasingly targeted for electrification using high-temperature heat pumps (HTHPs) that can co-deliver process cooling. Cross-sector syntheses and extensive application surveys establish the technical envelope above 100°C and provide harmonized test methods, key performance indicators (KPIs), and integration patterns pertinent to food and beverage plants, while also reporting the performance ranges that govern feasibility at scale [1–3]. Within this landscape, transcritical CO_2 cycles are especially relevant to breweries because the natural refrigerant supports sanitary integration, high volumetric heating capacity, and efficient heat recovery when the gas cooler is carefully matched to process temperature profiles. Recent market activity underscores industrial readiness, with suppliers announcing HTHPs capable of 120°C outlet temperatures and product literature citing a supply of up to 122°C for industrial use [2,4,5].

* Corresponding author. Tel.: +34-915-422-800
E-mail address: linares@comillas.edu

Accordingly, technology and economic comparisons should rely on sector-consistent metrics—e.g., heating COP, combined COP, and the seasonal performance factor (SPF)—and on levelized-cost frameworks that distinguish the levelized cost of heat (LCOH) from levelized cost of storage (LCOS). These frameworks must internalize temperature lift, annual utilization hours, time-of-use electricity pricing, and grid carbon intensity, especially for hybrid configurations in which the HTHP supplies the base load while existing boilers cover peaks and contingencies [1–3,6]. At industrial scales, surveys and databases report commercial supply temperatures of 110–150°C and demonstrations up to 156°C, with COP decreasing as lift increases (e.g., ≈4.3–5.8 for $\Delta T \approx 35$ K and ≈2.1–2.5 for $\Delta T \approx 70$ K), enabling rapid delimitation of operating windows and integration needs [1,3].

Thermal energy storage (TES) is a key complement to HTHPs in breweries because batch operations and diurnal tariff signals create mismatches between heat supply and demand. Sensible TES options with demonstrated applicability in the 120–300°C window include pressurized water, mineral and synthetic thermal oils, and molten salts; materials reviews provide stability windows, corrosion issues, and thermo-physical properties that guide medium selection and tank design [7–9].

For peak shaving and tariff arbitrage, two electricity-to-heat storage families are particularly relevant: Joule-heated firebrick electro-thermal energy storage (ETES), which offer low standby losses and flexible charging, and pumped thermal energy storage (PTES), which broadens integration with heat pumps and the grid [8,10,11]. In heat-recovery loops, variable-temperature storage (VTS) increases the recoverable heat relative to isothermal storage, especially when pairing HTHPs with condenser and vapor-recompression sources commonly found in food processing [12,13].

From a cycle-architecture perspective, the transcritical CO_2 configuration with internal heat exchange (IHX), active high-side (gas-cooler) pressure control, and segmented gas coolers is prevalent for medium- to high-temperatures sink. The internal pinch in the gas cooler—stemming from the pronounced peak in CO_2 heat capacity near the pseudocritical region—sets the minimum approach temperatures and drives the optimization of the discharge pressure. Furthermore, adding an IHX tends to lower the optimal discharge pressure while raising the discharge temperature, which constrains material and lubricant selection. Experimental exergy/energy evaluations of high-temperature prototypes with IHX also inform optimum discharge pressures and sectioning for 90–140°C operation, which is directly transferable to brewery preheat and low-pressure steam services [14]. Efficiency can be improved by recovering expansion work with ejectors in process-water and air-conditioning service configurations, which is applicable when breweries exploit simultaneous cooling loads, for example, in wort chilling or cold utilities [15].

In water-heating service, transcritical CO_2 systems with an expansion ejector have demonstrated COP≈4.6 (50–90°C), reducing compressor work versus throttling and indicating potential gains for process-water duties. In parallel, non-CO_2 HTHPs using low-global warming potential (GWP) hydrofluoroolefins or hydrochlorofluoroolefins (HFO/HCFOs) continue to demonstrate 110–160°C sinks. However, practical limits are often set by lubricant and motor temperatures, as well as by volumetric heating capacity at high pressure ratios, making them more suited to the lower end of brewery requirements or to cascades [16]. Beyond vapor compression, a helium Stirling prototype (400 kW) has achieved sink temperatures of 140-190°C, with a capability of up to 200°C [17], while reversed-Brayton developments indicate advantages over vapor compression when supply temperatures exceed 200°C [18].

Component-level advances underpin reliable operation at elevated temperature and pressure. Printed-circuit heat exchangers (PCHEs) and mini-channel gas coolers/recuperators provide high compactness and low approach temperatures across the pseudo-critical region. Recent experiments offer correlations for supercritical CO_2 in zigzag PCHEs, aiding design within this challenging regime [19]. Lubricant selection and management are non-trivial because miscibility and viscosity significantly impact supercritical CO_2 heat transfer and pressure drop. Reviews of the behavior of synthetic lubricants such as Polyalkylene glycol (PAG) and polyolester (POE) in gas coolers provide design guidance and highlight interactions that influence part-load stability, making lubricant selection and part-load control critical [20].

Successful brewery integration hinges on pinch-based targeting and thermal matching between the natural CO_2 temperature glide and the T–Q curves of water and thermal-oil circuits. Segmenting the gas cooler enables a higher-temperature oil loop (often used for indirect steam generation or kettle heating) to be run in parallel with a lower-temperature process-water loop, up to 90°C, thereby minimizing cumulative approach temperatures and exergy losses [21,22].

Operating modes that exploit synchronous cold-and-hot production—e.g., cooling the wort while charging the oil loop and preheating brewery hot water—maximize the combined COP [1–3]; conversely, heat-only operation on tempered sources (returns, ambient air/water) reduces instantaneous COP, which motivates the use of TES and optimized part-load control [2]. Seasonal increases in inlet-water temperature elevate the optimal gas-cooler (discharge) pressure and can increase the risk of high-pressure trips if not managed [21,22].

Operationally, transcritical CO_2 deployments must manage several risks: approach-temperature control across segmented gas coolers, stability when recuperators are present (internal pinch), thermal matching to oil–water temperature glide, high-pressure trips in hot seasons [21,22], and compliance with explosion risks standards (ATEX) and safety constraints in thermal-oil circuits at 250–300°C used for indirect steam. Mitigations include predictive control of gas-cooler/discharge pressure, adiabatic or evaporative assistance in summer, appropriate water treatment, and periodic cleaning-in-place (CIP) of heat exchangers, as well as protective instrumentation matched to the oil system's temperature class. In addition to pinch management, designers must consider compressor motor and oil temperature limits (with IHX) and water-quality effects (fouling/biofouling).

Early sectoral deployments illustrate feasibility and adoption pathways. In the UK, a major brewery is replacing site steam with a 90°C district-hot-water network supplied by ammonia HTHPs, validating the shift from steam to high-temperature hot-water where processes allow [23]. In parallel, a pilot 130°C steam heat pump at a regional brewer has reported substantial emissions and operating-cost reductions, signaling the near-term readiness of high-temperature electrification for kettle and pasteurization services; these demonstrations provide a bridge to CO_2-based HTHPs that can meet brewery-specific integration needs while leveraging natural refrigerants and tight thermal matching to process duties [24,25].

Building on this context, a high-temperature heat pump has been designed for integration into a brewery with an annual production capacity of 5.85 million hL. The heat pump has been designed to meet the full cooling demand of the wort (9.2 MW_{th}), heating up the process water and producing steam (3.5 barg) at variable load depending on the inlet-water temperature. The system replaces the existing ammonia chiller used for wort cooling (eliminating the condenser water requirement) and lowers the boilers' natural gas demand.

The novelty of this work lies in a brewery-specific integration architecture that transforms a single transcritical CO_2 unit into a tri-service retrofit providing wort cooling, inlet-water heating, and high-temperature thermal-oil charging for indirect steam generation. This is achieved via a split gas cooler configuration, comprising a dedicated oil heater and a process-water heater, together with a recuperator. This layout recovers process cooling as both inlet-water heating and a high-temperature energy stream. Unlike recent studies focusing on direct steam generation [26-28], this approach implements an indirect steam-side coupling via a thermal-oil loop with storage [7,8,13] to better manage the intermittency inherent to brewery steam demand.

Furthermore, beyond typical performance studies of simultaneous heating/cooling in food processing [29] or broad sectoral electrification and integration assessments [3,30,31], this contribution couples the integration concept with a detailed off-design operation framework. By utilizing turbocompressor performance maps to schedule rotational speed across seasonal inlet-water variations, the study provides a site-grounded retrofit design and quantifies its viability through annual application-consistent KPIs (seasonal COP, annual energy balance, and levelized cost/payback) [3,6].

2. Methods

Figure 1 illustrates the current factory layout. Boilers produce steam at 3.5 barg and hot wort. Cold water (89 m^3/h) from the distribution network is cooled to 3°C in an ammonia chiller before entering a recuperator that cools 90 m^3/h of wort from 98°C to 10°C. The boilers are fired mainly with natural gas (13.5 MW) and renewable fuels (biomass and self-produced biogas). The process operates 6,500 hours per year.

Figure 2 presents the proposed solution, which consists of a high-temperature heat pump operating with carbon dioxide (R744) in a reverse transcritical Rankine cycle. The heat pump integrates the three thermal demands of the process: the gas cooler is split into two units with heat recovery between them. The high-temperature unit (OHX) heats a thermal-oil loop to manage the intermittency in the steam production, whereas the low-temperature unit (PWHX) heats the water coming from the municipal network. The evaporator of the heat pump (WHX) cools the wort. A recuperator (REC) preheats the working fluid before the compressor inlet, reducing its temperature to the desired value before the PWHX inlet. In this configuration, the heat pump replaces the ammonia chiller and the recuperator in the current layout, as well as part of the heat supplied by the boilers.

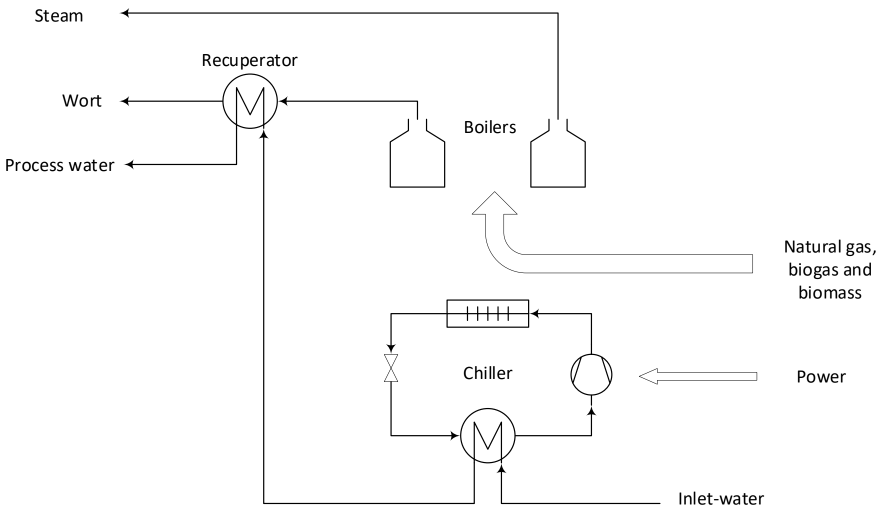

Figure 1. Current layout.

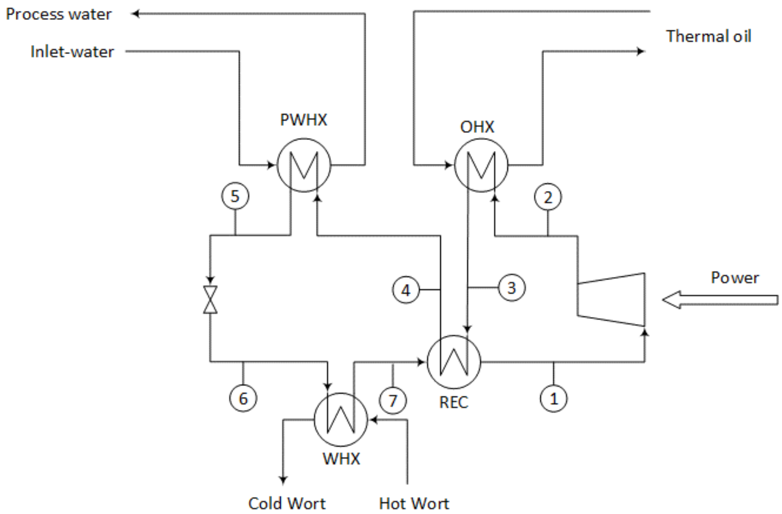

Figure 2. Proposed high-temperature heat pump.

The boundary conditions at the design point are summarized at Table 1. The inlet-water temperature varies over the year from 8 to 24ºC; 10°C has been adopted as the design-point value because it is the most frequently observed temperature over the annual distribution. The heat-pump model has been implemented in Engineering Equation Solver (EES) [32], using its internal routines to determine the thermal conductance (UA) of the heat exchangers. After sizing the UA at the design point, off-design simulations have been performed with UA held constant to obtain the performance of the heat exchangers at different inlet-water temperatures. This hypothesis is based on the model developed by Patnode [33], where UA depends on the mass flow rate in each stream of the heat exchanger. A turbomachinery compressor has been selected, whose rotational speed and preliminary design have been determined using the Baljé method [34] at the design point. The detailed compressor design has been completed with the commercial code COMPAL™ from NREC, and the geometries of the individual components have been obtained. COMPAL™ uses real-fluid properties and includes the loss-based Aungier model, which was used to estimate the compressor efficiency.

Because variations in inlet-water temperature materially change the required compressor pressure ratio—and would otherwise degrade compressor efficiency—a variable-speed control strategy has been implemented to adjust rotational speed is adjusted and maintain near-optimal efficiency across the full inlet-water temperature range.

Table 1. Boundary conditions

Parameter	Value	Unit
Wort inlet temperature	98	°C
Wort outlet temperature	10	°C
Wort flow rate	90	m^3/h
Inlet-water temperature	8–24	°C
Process-water outlet temperature	90	°C
Process-water flow rate	89	m^3/h

The levelized cost of energy (*LCOE*) has been assessed [35], considering as the useful energy the heat delivered to the thermal-oil loop for steam generation (Q_{OHX}), as defined in Eq. (1). In this equation, *INV* denotes total investment; *CRF* is the capital recovery factor, given by Eq. (2); γ is the maintenance factor (5%); *W* is the annual electricity consumed by the compressor and T_e is the electricity price (75 €/MWh).

$$LCOE = \left(\frac{INV}{Q_{OHX}}\right) \cdot (CRF + \gamma) + \frac{W \cdot T_e}{Q_{OHX}} \tag{1}$$

$$CRF = \frac{wacc \cdot (1+wacc)^N}{(1+wacc)^N - 1} \tag{2}$$

Capital costs have been estimated using correlations from [36] and escalated to 2024 prices with the Chemical Equipment Purchase Index (CEPI; 567.5 in 2017 and 798.8 in 2024). A factor of 1.3 has been applied to consider installation costs (assuming retrofits in an existing facility), whereas indirect costs have been assumed to be 25% of the investment [35]. The weighted average capital cost (wacc) was set to 7.5%, and the project's lifespan to 25 years

The costs of the proposed system are compared with a reference case that uses electricity for the ammonia chiller and gas for the boiler. This comparison allows standard profitability metrics such as NPV and payback period to be evaluated. Eq. (3) gives the NPV, treating the OPEX of the reference case ($OPEX_{conv}$) as a saving and combining it with the LCOE. Eq. (4) defines the OPEX of the reference case, assuming a boiler efficiency (η_{boiler}) of 90%, a gas price (T_g) as 40 €/MWh, and a carbon tax (T_{CO2}) as 16 €/MWh (nominal escalation rate for carbon tax taken as 0%). The electricity consumption of the ammonia chiller ($W_{chiller}$) is calculated assuming a COP of 3.

$$NPV = (OPEX_{conv} - LCOE) \cdot \left(\frac{Q_{OHX}}{CRF}\right) \tag{3}$$

$$OPEX_{conv} = \frac{\left(\frac{Q_{OHX}}{\eta_{boiler}}\right) \cdot (T_g + T_{CO2}) + W_{chiller} \cdot T_e}{Q_{OHX}} \tag{4}$$

3. Results

Figure 3 shows the p-h diagram at the design point, where the heat released at the PWHX is 8.28 MW; 4.73 MW at the OHX and the heat absorbed from the wort is 9.21 MW; the compressor requires 3.8 MW. Figure 4 presents the T-Q diagrams of the heat exchangers at the design point. The thermal conductance results in 384 kW/K for the WHX; 843 kW/K for the PWHX; 153 kW/K for the REC and 382 kW/K for the OHX. Figure 5 gives the mass flow rate evaluation of CO_2 and thermal oil, showing a nearly constant behavior. As the mass flow rates of wort and process water are constant, the thermal conductance remains constant, as it has been assumed.

A single-stage compressor has been selected, using the Baljè method, with a nominal rotational speed of 52,000 rpm; the main geometry parameters at the design point (inlet-water temperature 10°C) are represented in Figure 6.

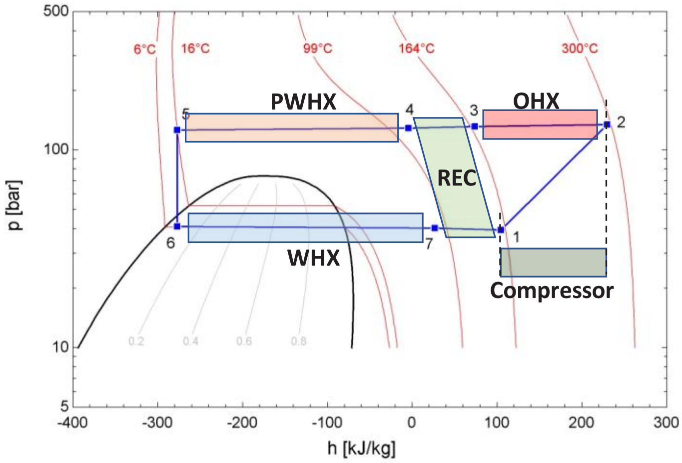

Figure 3. P-h diagram at the design point.

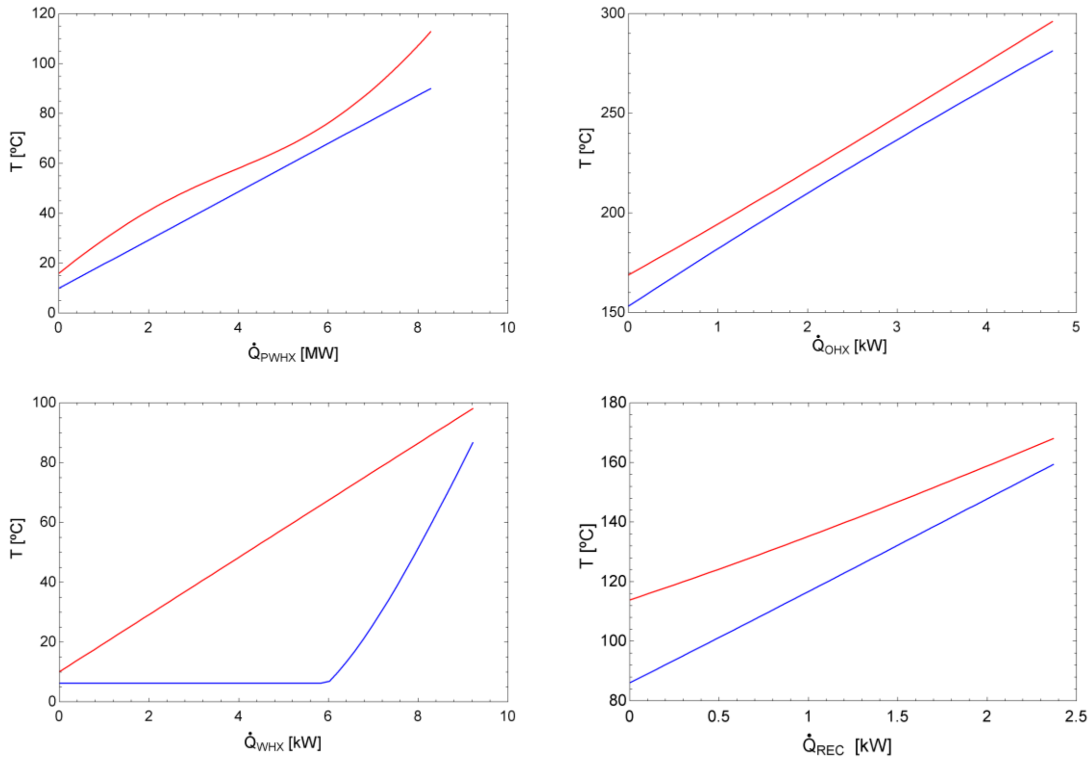

Figure 4. T-Q diagrams at de design point.

The variation of the inlet-water temperature results in the operation of the heat pump in off-design mode. Maintaining the boundary conditions in the wort, the thermal oil enters OHX at temperatures between 136°C and 155°C and returns to storage at 343°C to 269°C. The inlet-water enters the system at 8°C to 24°C and is heated to 90°C. But invariantly, the wort is cooled from 98°C to 10°C, removing 9.2 MW_{th}. To analyze the off-design mode, the efficiency map of the compressor has been obtained and is presented in Figure 7, where also pressure ratio is shown as a function of rotational speed and mass flow rate.

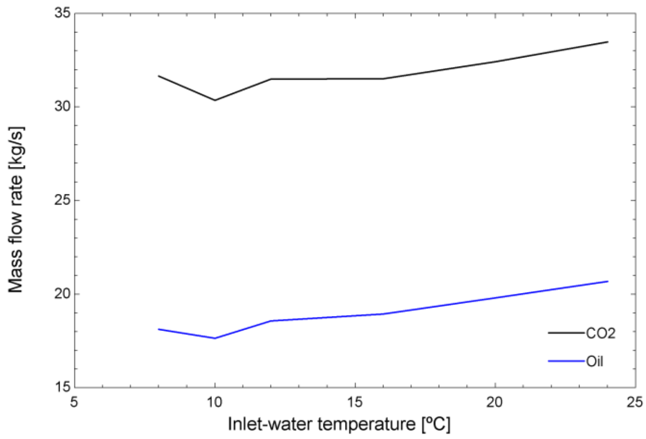

Figure 5. Mass flow rate variation in the working fluid of the heat pump and the thermal oil depending of the inlet-water temperature.

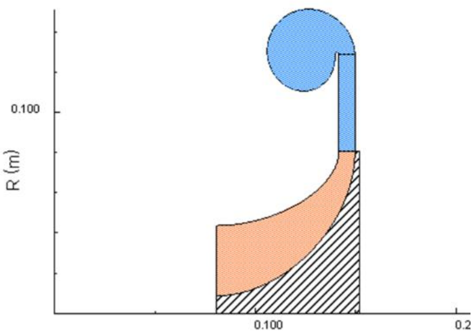

Figure 6. Geometry of the single-stage compressor.

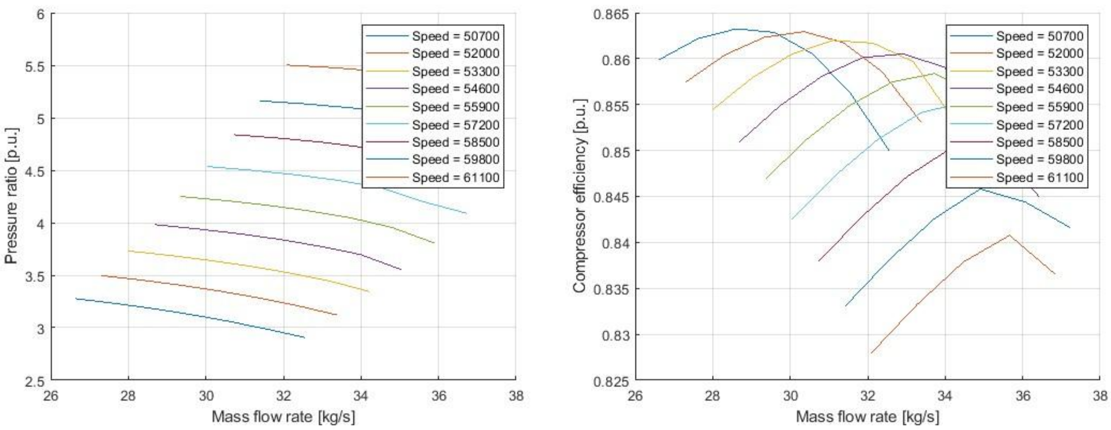

Figure 7. Compressor pressure ratio and efficiency maps

Owing to variations in the required pressure ratio, a variable-speed control strategy has been implemented whereby rotational speed is adjusted as a function of the inlet-water temperature. Using the derived performance maps, the rotational-speed for each inlet-water temperature and the corresponding predicted efficiency have been obtained, as shown in Figure 8.

Figure 9 shows the heat-pump performance (heat duties and COP) as a function of the inlet-water temperature. The COP is defined to include heating and cooling effects, specifically, heat at the PWHX, OHX and WHX as useful output.

An annual simulation of the heat pump across the inlet-water temperature distribution produces 40.6 GWh delivered to the thermal-oil loop, 50.7 GWh to process water, and 59.9 GWh of heat removed from the wort, with 31.4 GWh of power consumed by the compressor, corresponding to a seasonal COP of 4.82. For comparison, the boilers currently supply 87.8 GWh of natural-gas heat.

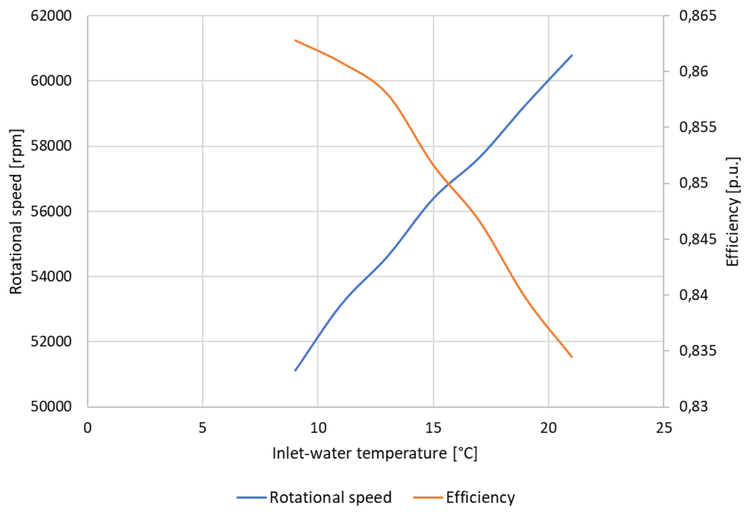

Figure 8. Rotational speed and compressor efficiency as a function of inlet-water temperature

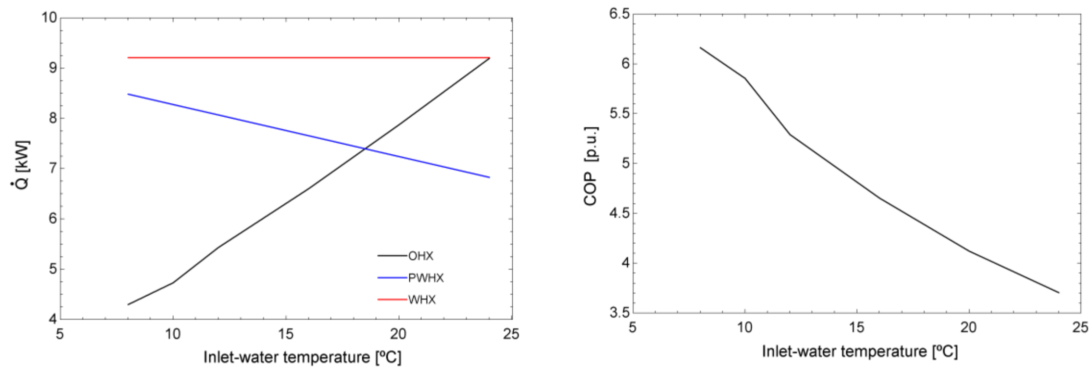

Figure 9. Performance of HTHP as a function of inlet-water temperature.

Table 2 summarizes the breakdown of the investment, resulting in an annual maintenance cost of 292,416 €, when 5% of the total investment is assumed. Figure 10 illustrates the breakdown of the levelized cost of energy for the heat pump, which results in 78.15 €/MWh. It is noticeable that compressor consumption accounts for more than 74% of the LCOE, whereas the CAPEX contributes less than 17%. This cost structure reflects the premium associated with electricity procured under guarantees-of-origin contracts relative to conventional tariffs. As a reference, the current OPEX for the ammonia chiller and the natural gas boilers results in 81.75 €/MWh, yielding a payback period of 14.7 years.

Table 2. Investment breakdown.

Component	Cost [$€_{2024}$]
OHX	6,174
PWHX	11,218
WHX	6,196
REC	3,102
Compressor	3,572,272
Installation and piping	1,079,689
Indirect costs	1,169,663
TOTAL Investment	5,848,314

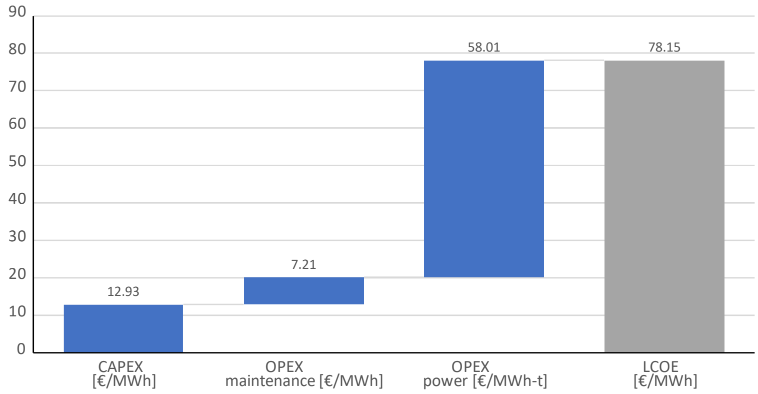

Figure 10. Levelized cost of energy breakdown of the heat pump.

In order to reduce the payback period, an optimized scenario has been considered, based on the following assumptions: reduction of the wacc to 5%, design capacity doubled, and reduction of the maintenance factor to 3%. Table 3 compares the results of both scenarios, showing a significant improvement in economic feasibility of the optimized scenario. This reduction is explained by the lower wacc (a 21% reduction in the CRF) and the higher scale, which reduces the specific investment from 450 € to 297 € per kW of installed heat to the sink (OHX +WPHX). The lower specific investment and the lower maintenance factor considered in the optimized scenario, result in a 60% reduction in maintenance OPEX.

Table 3. Investment breakdown.

Parameter	Baseline scenario	Optimized scenario
CAPEX [€/MWh]	12.93	6.76
OPEX maintenance [€/MWh]	7.21	2.86
OPEX power [€/MWh]	58.01	58.01
LCOE [€/MWh]	78.15	67.63
Payback period [years]	14.7	5.31

Figure 10 shows that the electricity price has a strong impact on the LCOE. To quantify this effect, a sensitivity analysis with a ± 20% variation in electricity price was carried out for both scenarios, as shown in Figure 11. In the baseline scenario, the highest electricity price considered is 81.22 MWh, which is 8.3 % higher than the baseline value. In the optimised scenario, a 20 % increase in electricity price still yields a payback period of 10 years. In this optimized scenario acceptable performance is maintained even if the operating hours are reduced to 5380 hours with an electricity price of 75 €/MWh.

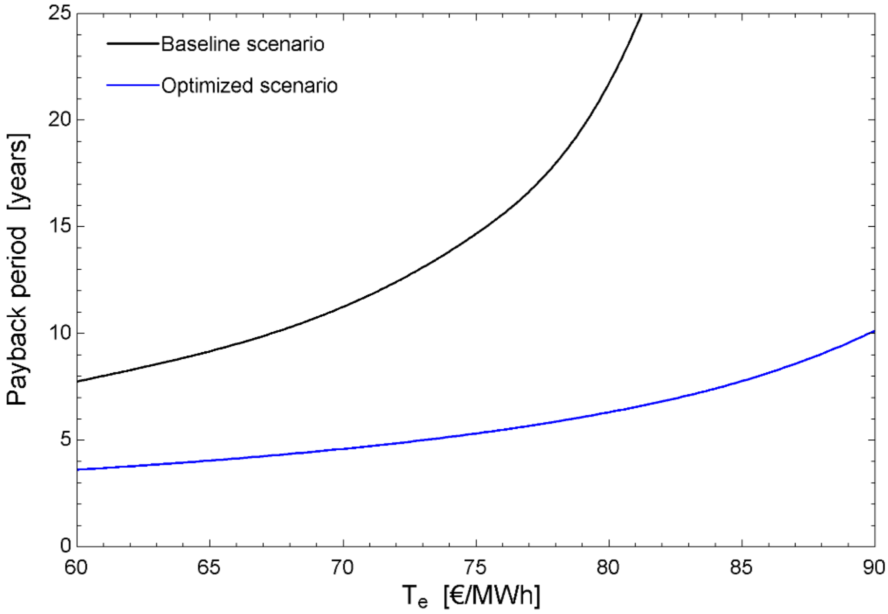

Figure 11. Sensitivity analysis of payback period to electricity price.

Avoided emissions attributable to the heat pump arise from displacement of natural gas fuelling the boiler by the 40.6 GWh delivered to the thermal-oil loop; heat delivered to process water is excluded because, in the current configuration, it is recovered from the wort. Assuming a boiler efficiency of 90% and a CO_2 factor for natural gas of 0.182 kg CO_2/kWh-HHV, the avoided emissions are 8,346 t CO_2. Considering a production of 5,850,000 hL of wort, the ratio of avoided emissions results in 1.43 kg CO_2/hL of wort.

4. Conclusions

This study demonstrates the technical feasibility of electrifying medium-temperature heat in a large brewery by integrating a transcritical CO_2 HTHP operating on a reverse Rankine cycle. The proposed system replaces the ammonia chiller used for wort cooling and recovers the extracted heat to supply part of the steam duty via a thermal-oil loop, while also heating process water to 90°C. A turbomachinery compressor with variable-speed control maintains high efficiency across seasonal inlet-water temperatures (8–24°C). At the design point, the heat pump has been sized to deliver 8.28 MW to process water and 4.73 MW to thermal oil while removing 9.21 MW from the wort.

Economic results indicate near-term competitiveness. The baseline LCOE is 78.15 €/MWh versus 81.75 €/MWh for the incumbent configuration. An optimized case (lower wacc, doubled capacity, reduced maintenance) lowers LCOE to 67.63 €/MWh and shortens payback from 14.7 to 5.31 years. The HTHP avoids 8,346 t CO_2 per year, equivalent to 1.43 kg CO_2 per hL of wort. Overall, transcritical CO_2 HTHPs emerge as a practical, near-term pathway for deep electrification of brewery heat with strong energy, cost, and emissions performance.

Acknowledgements

Authors acknowledge to Rafael Mariño Chair on New Energy Technologies and Repsol Foundation Chair in Energy Transition of Comillas Pontifical University for its support.

References

[1] Arpagaus, C.; Bless, F.; Uhlmann, M.; Schiffmann, J.; Bertsch, S.S. (2018). High temperature heat pumps: Market overview, state of the art, research status, refrigerants, and application potentials. Energy 152, 985–1010. https://doi.org/10.1016/j.energy.2018.03.166

[2] IEA HPT TCP (2024). Annex 58 – High-Temperature Heat Pumps. Final Report. Heat Pump Centre. Report No. HPT-AN58-1. ISBN 978-91-89896-81-9. https://doi.org/10.23697/2qxe-av87

[3] Schlosser, F.; Jesper, M.; Vogelsang, J.; Walmsley, T.G.; Arpagaus, C.; Hesselbach, J. (2020). Large-scale heat pumps: Applications, performance, economic feasibility and industrial integration. Renewable & Sustainable Energy Reviews 133, 110219. https://doi.org/10.1016/j.rser.2020.110219

[4] MAN Energy Solutions. (2024). MAN heat pumps — Vapor compression cycle (VCC) (brochure, PDF). Retrieved October 29, 2025, from https://www.man-es.com/docs/default-source/document-sync/man-heat-pump-hpu328c592b5d584f9eba47f4b6bed3574e.pdf

[5] Triveni Turbines. (2025). Triveni Turbines unveils India's First CO_2-Based Heat Pump (press release, PDF). Retrieved October 29, 2025, from https://www.triveniturbines.com/wp-content/uploads/2025/08/TTL_PressRelease_HeatPump.pdf

[6] Gilbert, T.; Menon, A.K.; Dames, C.; Prasher, R. (2023). Heat source and application-dependent levelized cost of decarbonized heat. Joule 7(1), 128–149. https://doi.org/10.1016/j.joule.2022.11.006

[7] Miró, L.; Gasia, J.; Cabeza, L.F. (2016). Thermal energy storage (TES) for industrial waste heat (IWH) recovery: A review. Applied Energy 179, 284–301. https://doi.org/10.1016/j.apenergy.2016.11.097

[8] Wolde, I.; Cardemil, J.M.; Escobar, R. (2024). Compatibility assessment of thermal energy storage integration into industrial heat processes. Journal of Cleaner Production 440, 140932. https://doi.org/10.1016/j.jclepro.2024.140932

[9] Caraballo, A.; Galán-Casado, S.; Caballero, Á.; Serena, S. (2021). Molten Salts for Sensible Thermal Energy Storage: A Review and an Energy Performance Analysis. Energies 14, 1197. https://doi.org/10.3390/en14041197

[10] Stack, D.C.; Forsberg, C. (2019). Performance of firebrick resistance-heated energy storage for industrial heat applications and round-trip electricity storage. Applied Energy 254, 113660. https://doi.org/10.1016/j.apenergy.2019.03.100

[11] Sharma, M.; Mortazavi, M. (2023). Pumped thermal energy storage: A review. International Journal of Heat and Mass Transfer 213, 124286. https://doi.org/10.1016/j.ijheatmasstransfer.2023.124286

[12] Walmsley, T. G., Lincoln, B. J., Padullés, R., & Cleland, D. J. (2018). Process and utility systems integration and optimisation for ultra low energy milk powder production. Energy, 140, 152–167. https://doi.org/10.1016/j.energy.2017.04.142

[13] Walmsley, T. G., Walmsley, M. R. W., Neale, J. R., Atkins, M. J. (2014). Integration of industrial solar and gaseous waste heat into heat recovery loops using constant and variable temperature storage. Energy, 75, 53–67. https://doi.org/10.1016/j.energy.2014.01.103

[14] Mateu Royo, C., Navarro Esbrí, J., & Molés, F. (2019). Experimental exergy and energy analysis of a novel high-temperature heat pump with scroll compressor for waste heat recovery. Applied Energy, 253, 113504. https://doi.org/10.1016/j.apenergy.2019.113504

[15] Zhu, Y., Huang, Y., Li, C., Zhang, F., & Jiang, P. X. (2018). Experimental investigation on the performance of a transcritical CO_2 ejector expansion HP water heater system. Energy Conversion and Management, 167, 931–942. https://doi.org/10.1016/j.enconman.2018.04.081

[16] Zhou, D.; Meng, Z.; Liu, Y.; Dong, S.; Zhang, F.; Ding, C.; Huo, Z.; Wang, M. (2023). Theoretical study of low GWP refrigerants (R1224yd(Z), R1223zd(E), R1336mzz(Z)) in HTHP systems. International Journal of Low Carbon Technologies, 18, 881–886. https://doi.org/10.1093/ijlct/ctad059 (OUP Academic)

[17] Høeg, A.; Løver, K.; Asphjell, T.-A.; Lümmen, N. (2023). Performance of a new ultra-high temperature industrial heat pump (Stirling cycle, helium). 14th IEA Heat Pump Conference, Chicago.

[18] Kim, J.-S.; Chung, I.-H.; Kim, T.-S.; Song, C.-H. Thermal Performance Design and Analysis of Reversed Brayton Cycle Heat Pumps for High-Temperature Heat Supply. Energies 2024, 17, 2953. https://doi.org/10.3390/en17122953

[19] Jin, F.; Yuan, D.; Chen, D.; Hu, L.; Huang, Y.; Bu, S. (2023). Cooling heat transfer of supercritical CO_2 in zigzag printed-circuit mini-channels. International Journal of Heat and Mass Transfer, 215, 124538. https://doi.org/10.1016/j.ijheatmasstransfer.2023.124538

[20] Wenjie Xu, Minxia Li, Yang Li, Jun Zhao, A comprehensive review of the effect of lubricant on the flow characteristics of supercritical CO2 during cooling, International Journal of Refrigeration, Volume 133, 2022, Pages 145-156, https://doi.org/10.1016/j.ijrefrig.2021.10.018.

[21] Chen, Y. G. (2016). Pinch point analysis and design considerations of CO_2 gas cooler for heat pump water heaters. International Journal of Refrigeration, 69, 136 – 151. https://doi.org/10.1016/j.ijrefrig.2016.05.003

[22] Ye, Z., Wang, Y., & Song, Y. (2020). Optimal discharge pressure in a transcritical CO_2 HP water heater with IHX based on pinch point analysis. International Journal of Refrigeration, 118, 12–20. https://doi.org/10.1016/j.ijrefrig.2020.06.003

[23] GEA supplies HEINEKEN UK with heat pump solution for Manchester site. 27 Jul 2023 https://www.gea.com/en/news/corporate/2023/gea-supplies-heineken-with-heat-pumps/

[24] European Heat Pump Association. Beer brewed with pump power https://ehpa.org/heat-pump-stories/beer-brewed-with-pump-power/

[25] The guardian. Brewer to cut emissions by making beer using a heat pump in UK first. https://www.theguardian.com/food/2024/oct/03/brewer-to-slash-emissions-by-making-beer-using-a-heat-pump-in-uk-first

[26] Ma, X., Du, Y., Zhao, T., Zhu, T., Lei, B., & Wu, Y. (2024). A comprehensive review of compression high-temperature heat pump steam system: Status and trend. International Journal of Refrigeration, 164, 218–242. https://doi.org/10.1016/j.ijrefrig.2024.04.024

[27] Chen, J., Guo, C., Feng, C., Qu, X., Tan, S., & Jiang, Y. (2025). Research of CO_2 high temperature heat pump for industrial steam generation with data center heat source. International Journal of Refrigeration, 173, 185–200. https://doi.org/10.1016/j.ijrefrig.2025.02.014

[28] Li, S., Song, Y., Chang, T., Yu, Q., Zhang, Y., & Cao, F. (2025). Revolutionizing 300 °C industrial steam with a novel transcritical carbon dioxide heat pump system: Thermodynamic and configuration analyses. Energy Conversion and Management, 346, 120556. https://doi.org/10.1016/j.enconman.2025.120556

[29] Dasi, K., Singh, S., Guruchethan, A. M., Maiya, M. P., Hafner, A., Banasiak, K., & Nekså, P. (2020). Performance evaluation of ejector based CO_2 system for simultaneous heating and cooling application in an Indian dairy industry. Thermal Science and Engineering Progress, 20, 100626. https://doi.org/10.1016/j.tsep.2020.100626

[30] Dumont, M., Wang, R., Wenzke, D., Blok, K., & Heijungs, R. (2023). The techno-economic integrability of high-temperature heat pumps for decarbonizing process heat in the food and beverages industry. Resources, Conservation and Recycling, 188, 106605. https://doi.org/10.1016/j.resconrec.2022.106605

[31] Liu, Z., Hu, B., Wu, D., & Wang, R. (2025). Electrification and decarbonization in global brewing industry driven by industrial heat pumps. Energy, 325, 136184. https://doi.org/10.1016/j.energy.2025.136184

[32] Engineering Equation Solver (https://fchartsoftware.com/ees/). Accessed on October 27, 2025.

[33] Patnode, A.M. (2006). Simulation and Performance Evaluation of Parabolic Trough Solar Power Plants, Master thesis dissertation, University of Wisconsin-Madison. https://minds.wisconsin.edu/handle/1793/7590

[34] Baljè, O.E. (1981). Turbomachines: A guide to design, selection and theory. Wiley.

[35] Bejan, A. (1997). Construction Costs and Design Economics. John Wiley & Sons.

[36] Weiland NT., Lance BW., Pidaparti SR., SCO2 Power cycle component cost correlations from DOE data spanning multiple scales and applications, Proceedings of ASME Turbi Expo 2019: Turbomachinery Technical Confrence and Exposition GT2019, June 17-21, 2019, Phoenix, Arizona, USA